JOURNAL OF MATERIALS SCIENCE 22 (1987) 1790–1798

The peel strengths of diffusion bonded joints between clad Al-alloy sheets

D. V. DUNFORD, P. G. PARTRIDGE
Materials and Structures Department, Royal Aircraft Establishment, Farnborough, Hampshire GU14 6TD, UK

Solid-state diffusion bonded joints were produced between silver-coated clad Al-alloy sheets. The alloys were based upon the systems Al–Zn–Mg (7010 alloy) and Al–Cu (2024 and Supral 220 alloys). The corresponding peel strengths of the joints in these alloys were 61, 45 and 42 N mm^{-1} in the solution heat treated state and 34, 12 and 48 N mm^{-1} in the aged state. At 480° C corresponding peel strengths were 2.4, 2.5 and 1.7 N mm^{-1}. The mechanism of peel fracture in the peel test and the possibility of combining diffusion bonding with superplastic forming are discussed.

1. Introduction

The combination of superplastic forming with diffusion bonding (SPF/DB) has led to substantial cost and weight savings for titanium aerospace structures [1]. Since a monolithic diffusion bonded joint with parent metal strength is readily obtained between titanium alloy sheets, the joints can withstand the peel stresses imposed during SPF at 850 to 930° C.

Although superplastic forming of Al–alloys is well-established [2] the diffusion bonding stage is made difficult by the hard stable surface oxide film which acts as a barrier to diffusion [3, 4]. The oxide film may be fragmented and dispersed by large deformations [3, 4] or by the formation of liquid phases at the bond interface [3, 5] and by soft interface foils or coatings [3, 4, 6].

Recent work has shown that diffusion bonded joints with high shear strengths can be produced between clad Al-alloy sheets if the sheet surfaces are first coated with silver [7]. Silver oxide is unstable above about 190° C and the silver surfaces could be bonded at ~300° C and the silver removed from the bond interface by diffusion at the solution heat treatment temperature. Since there is a dearth of peel strength data for diffusion bonded joints further tests were carried out to determine the peel strength at room temperature and at 480° C, which is about the minimum superplastic forming temperature for Al–alloys [8]. The results of these tests are described in this paper.

2. Experimental technique

The three aluminium alloys bonded were 2024, Supral 220 and 7010 with the compositions given in Table I; the first two alloys were based on the Al–Cu system and the third alloy on the Al–Zn–Mg system. The alloys were in the form of 1.6 to 3.5 mm thick clad sheet with clad layers on each surface of approximate thickness 35 μm (2024), 140 μm (Supral 220) and 120 μm (7010). Test-piece blanks 100 mm long and 18 mm wide were cut from each sheet with the long axis parallel to the sheet rolling direction. Prior to bonding one surface over a 20 mm length at one end of the blank was polished to a 1 μm diamond surface finish before ultrasonic cleaning in acetone and washing in alcohol. The polished surface was r.f. sputter cleaned and ion plated with a 1 μm thick silver layer as described elsewhere [9].

Diffusion bonding was carried out in an argon atmosphere at a maximum temperature of 280° C under a pressure of 120 MPa. A bonding cycle time of approximately 45 min produced a 10 to 15% thickness reduction across the bonded joint. A section through a joint showing the silver and clad layers is shown in Fig 1a. After bonding the test pieces were heated at 480° C and the unbonded ends were bent through an angle of 90° to form a T-peel test piece as shown in Fig. 2. Test pieces were subsequently heat treated as indicated in Table I. The silver layers were removed by diffusion during solution heat treatment (Fig. 1b) and the residual silver concentration was 1.0 to 1.7 wt % [10]. The edge of the test piece in the bonded region was polished and lines 1 mm apart were scribed on the surface to enable the position of the crack to be observed during testing.

The tensile peel tests were carried out at constant cross-head speed of 0.8 mm min^{-1}.

Some peel strengths were measured using a single test piece which was fractured initially in the solution heat treated (SHT) condition (as shown in Fig. 3) before either ageing or heating to 480° C and peeling further to failure.

Micro-hardness was measured using a Vickers pyramid indenter under 9 and 20 g loads. Electron probe microanalysis was carried out on the 7010 bonded joints as described elsewhere [10].

3. Results

3.1. Peel strength

In the SHT state the peel strength at room temperature was greatest for the 7010 alloy at 61 N mm^{-1} (Table II). The values for 2024 and Supral 220 alloys

0022–2461/87 $03.00 + .12

TABLE I

Alloy	Composition (wt %)								Heat treatment	
	Cu	Mg	Zn	Fe	Zr	MN	Ge	Si	Solution heat treatment (SHT)	Ageing treatment
7010										
Alloy	1.7	2.3	6.0	–	0.11	–	–	–	16 h at 480° C	24 h at 120° C
Clad layer	–	–	1	–	–	–	–	–	Water quench	10 h at 172° C
SUPRAL 220										
Alloy	5.9	0.35	0.07	0.18	0.4	–	0.1	0.12	16 h at 520° C	16 h at 180° C
Clad layer	–	–	–	–	–	–	–	–	Water quench	
2024										
Alloy	4.4	1.5	–	–	–	0.6	–	–	16 h at 498° C	16 h at 190° C
Clad layer	0.1	–	0.1	0.7	–	–	–	–	Water quench	

were slightly lower at 45 and 42 N mm^{-1} respectively. A typical load–time curve is shown in Fig. 4; the load increased rapidly to a maximum value at A when crack growth began and remained almost constant at B until failure at C.

When a peel test was stopped in the constant load region, the deformation associated with crack growth was apparent in the polished surface at the edge of the test piece as shown for the 7010 alloy bond in Fig. 5a. The crack tip at A deviated from the bond interface at B and was associated with extensive plastic deformation which extended through the clad layer at C and into the parent alloy at D. In Supral 220 alternate slow and fast crack growth periods occurred and plastic deformation zones developed during the slow growth periods as shown at A and B in Fig. 5b; deformation in the parent alloy is visible at C. The variable crack growth rate led to a saw-toothed fracture surface as shown in Fig. 5c.

The ageing treatments increased slightly the peel strength of Supral 220 to 48 N mm^{-1}, but reduced the peel strength of 7010 and 2024 alloys to 34 and 12 N mm^{-1}, respectively (Table II). Aged test pieces fractured by rapid crack growth when the maximum load was reached and constant load plateaus were not observed. Under these conditions plastic deformation associated with crack growth was much less than in the SHT state and was confined to narrow regions very close to the bond interface.

The load–time curves obtained at 480° C were similar to the curves for aged test pieces at room temperature. The peel strengths at 480° C (Table II) were 2.4 N mm^{-1} (7010 alloy), 1.7 N mm^{-1} (Supral 220 alloy) and 2.5 N mm^{-1} (2024 alloy) and were proportional to the alloy concentration in the clad layer (Table III).

TABLE II

Alloy	Peel strength (N mm^{-1})		
	Tested at 22° C		Tested at 480° C
	SHT	Aged	SHT
7010	61	34	2.4
SUPRAL 220	42	48	1.7
2024	45	12	2.5

3.2. Fractography

The appearance of the fractures depended on heat treatment and test temperature. The fracture surface of the 7010 alloy fractured initially in the SHT condition and then in the aged condition is shown in Fig. 6a; the crack front in the SHT condition was very irregular as indicated by the dash line. A coarse dimpled fracture surface was characteristic of the SHT condition as shown at A in Figs 6a and b. A smooth fracture surface with discrete raised islands was

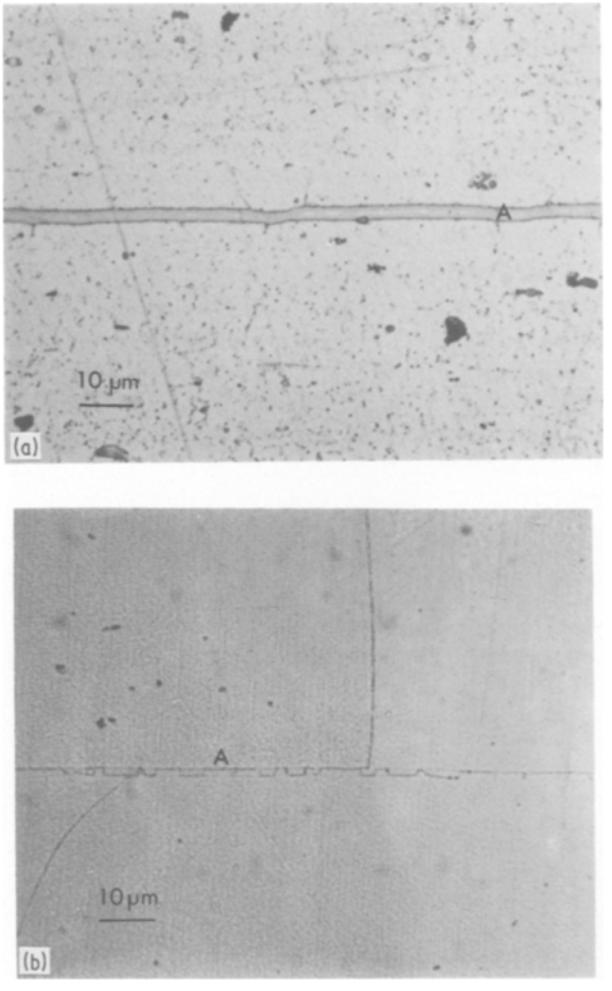

Figure 1 Diffusion bonded interface in 7010 alloy. (a) As bonded showing silver layers at A. (b) After SHT showing residual planar grain boundaries at A.

TABLE III

Alloy	Clad layer thickness (μm)	Hardness (kg mm^{-2})				Composition (at %)					
		SHT condition		Aged condition		Alloy			Bond interface after SHT		
		Alloy	Clad layer 20 μm from bond interface	Alloy	Clad layer 20 μm from bond interface	Cu	Zn	Mg	Cu	Zn	Mg
7010	120	192	136	217	145	0.68	2.47	2.57	0.12	1.36	0.67
SUPRAL 220	140	138	67	170	63	2.3	–	0.39	–	–	–
2024	35	170	150	183	176	1.76	–	1.67	–	–	–

characteristic of the aged condition as shown at B in Figs 6a and c. The fracture surface of the 7010 alloy fractured initially in the SHT condition at room temperature and then at 480° C is shown in Fig. 7a; an irregular crack front and coarse dimples are apparent in the room temperature fracture (Figs 7a to c). The fracture at 480° C was macroscopically flat but very finely dimpled (Figs 7b and d).

The peel fractures in the Supral 220 (Fig. 8) and 2024 alloys showed similar trends with ductile and cleavage type fractures in the SHT and aged conditions, respectively. Some very small ductile cusps could be resolved on the aged fractures at high magnification (Figs 7c and 8c). At 480° C the characteristic flat fractures were also obtained in Supral 220 (Fig. 9) and 2024 alloys, but there was no evidence of ductile cusps in the Supral fracture (Fig. 9b).

3.3. Microhardness

Microhardness values across the bonded joints are plotted in Fig. 10. The clad layers in all the alloys increased in hardness during solution heat treatment, but only the 2024 alloy clad layer increased in hardness during the ageing treatment (Fig. 10c). In the SHT condition the hardness near the bond interface decreased with increase in clad layer thickness. This decrease corresponded to the decrease in alloy content at the bond interface (Table III).

4. Discussion

In the present tests bonds in the SHT condition had peel strengths greater than 40 N mm^{-1}. The peel strengths reported [1] for Al-alloys roll bonded using soft 6061 Al-alloy interlayers in the SHT condition were lower at 22.9 N mm^{-1} for the 2024 alloy and 23.8 N mm^{-1} for the 7075 alloy. In the aged state meaningful peel strengths could not be obtained for these bonds. For comparison typical peel strengths reported for adhesive bonded Al-alloys and for Pb–Sn soldered joints are $\sim$8 N mm^{-1} [12, 13] and $\sim$35 N mm^{-1} [14], respectively.

After SHT the original bond interfaces, i.e. Ag/Ag and Ag/cladding, persisted as planar large angle boundaries [15] as shown in Fig. 1b. The normal solute depleted zones occurred in the boundaries after ageing [15]. The diffusion of silver and of alloying elements from the alloys, e.g. copper, magnesium and zinc, increased the alloy content and the hardness of the clad layers (Fig. 10, Table III), but the clad layer composition was always less than that of the parent alloy (Table III).

The hardness of the clad layers was dependent on the alloying elements present, on their diffusion rates and on the clad layer thickness. The diffusion rates relative to copper at the SHT temperature were Mg $\sim$ 2.3 $\times$ Cu and Zn $\sim$ 4 $\times$ Cu. This led to

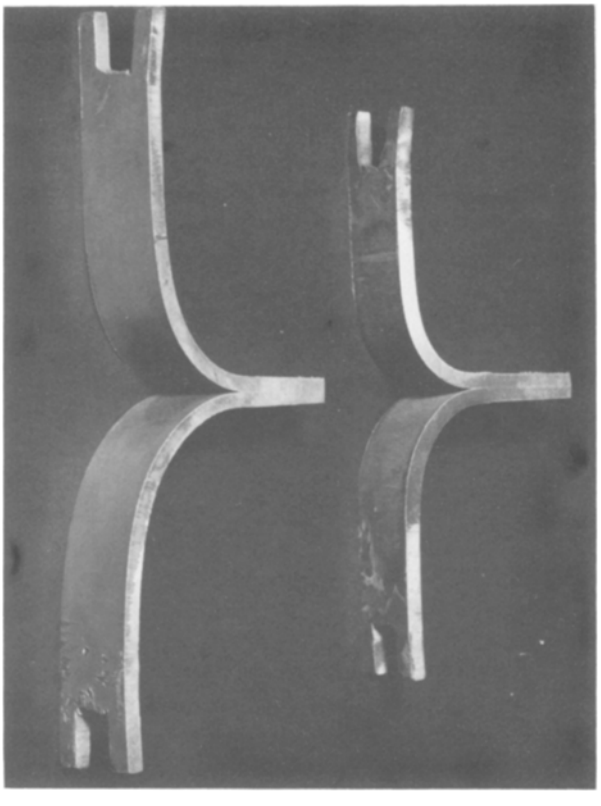

Figure 2 T-peel test pieces.

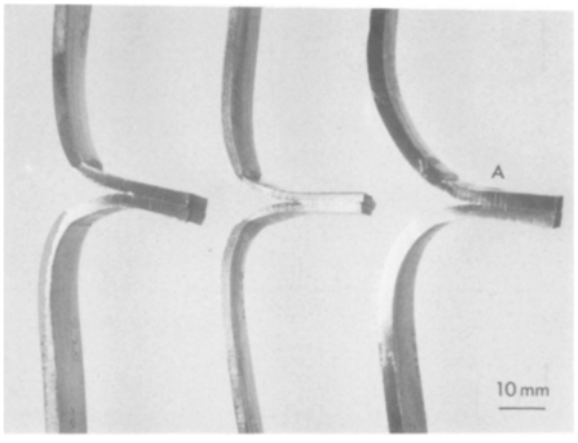

Figure 3 Test pieces after initial peel fracture in the SHT condition at room temperature.

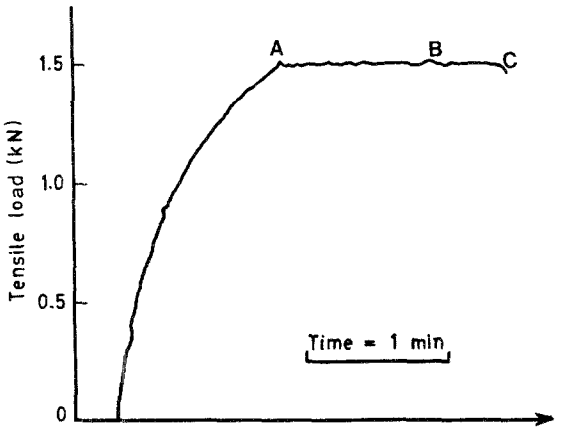

Figure 4 Tensile peel load against time curve for 7010 alloy in SHT condition.

decreasing hardness with increasing clad layer thickness in the Al–Cu alloys and for comparable clad layer thicknesses a greater hardness in the 7010 alloy clad layers than in the Supral 220 alloy clad layers. Age hardening and the greatest clad layer hardness was observed in the thinnest clad layer (alloy 2024) containing the highest copper content (Table III).

There was no direct relationship between peel strength and hardness of the clad layer alone (Figs 11 and 12). In the SHT condition the peel strengths were similar in the two Al–Cu alloys although they represented the extremes of the hardness range. The ageing treatment increased the clad layer hardness in the 2024 alloy but decreased the peel strength by 73%. Ageing had little effect on the hardness of the 7010 or Supral 220 clad layers, but led to a 44% reduction and zero reduction respectively in peel strength.

In all the alloys peel fractures at room temperature were related to the heat treatment condition. Ductile and limited ductility fractures were obtained in the SHT and aged conditions respectively. It is significant that flat fractures were obtained even at 480° C with (Figs 7a and c) or without (Fig. 9) very small ductile cusps. These low ductility fractures appeared to coincide with the planar boundaries near the bond interface. The above results suggest that the onset of this fracture mode in the aged condition was related to the increase in hardness of the alloy and of the clad layers relative to the solute depleted zone in the planar grain boundaries.

The T-peel test piece is widely used to measure the relative peel strengths of adhesive bonded joints [16]. The key factor in determining fracture under peel conditions is the bending moment at the crack tip which results in tensile loads across the joint [16]. When yielding of both the adhesive and the adherend was taken into account it was possible to predict the peel strength of an adhesive bonded Al-alloy joint [17]. The shear and peel strengths for diffusion bonded Al-alloy joints are over four times greater than the corresponding values for adhesive bonded joints [18, 19], and this leads to greater deformation of the diffusion bonded test pieces.

The effect of ageing on the peel strength of diffusion bonded joints can be explained in terms of the energy required to fracture a peel test piece. The energy provided by the cross-head displacement and load is used to produce:

1. two fracture surfaces,
2. micro-deformation around the crack tip (Fig. 5),
3. macro-deformation of the peel test piece (Fig. 3).

In the SHT condition at room temperature the energy was dissipated largely by plastic deformation in (2) and (3). The relative peel strengths of the joints were therefore proportional to the thickness and hardness of the clad layers (Figs 11 and 12). After ageing, (1) is

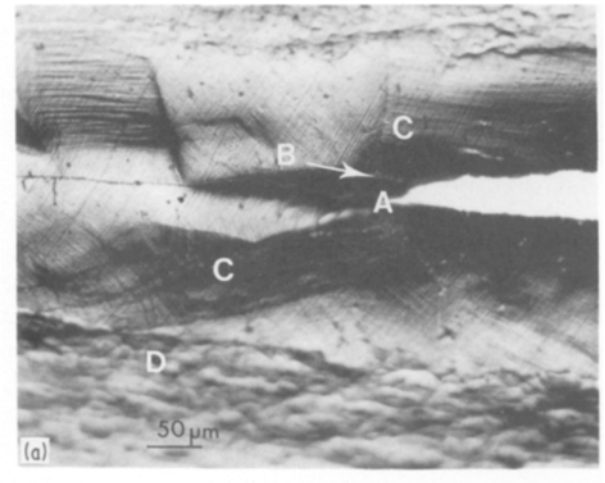

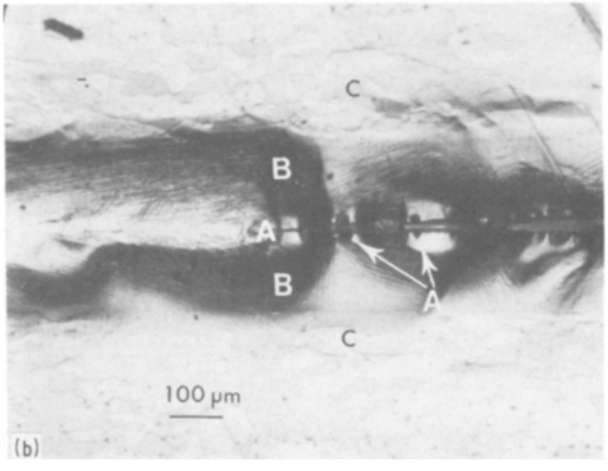

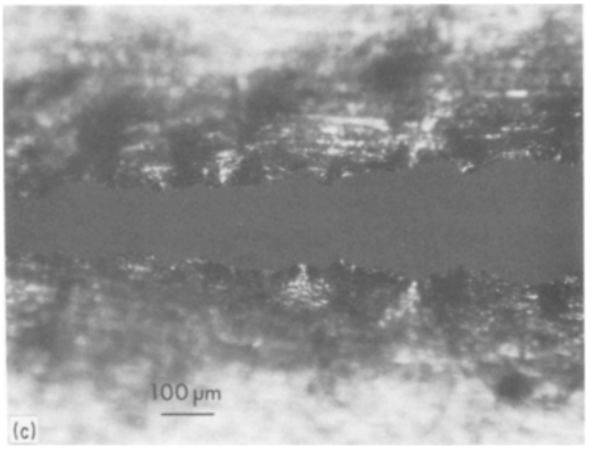

Figure 5 Deformation near peel fractures in (a) 7010 alloy (b and c) SUPRAL 220 alloy.

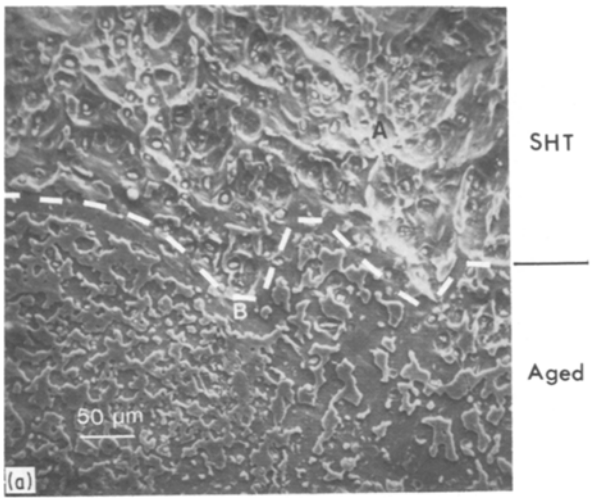

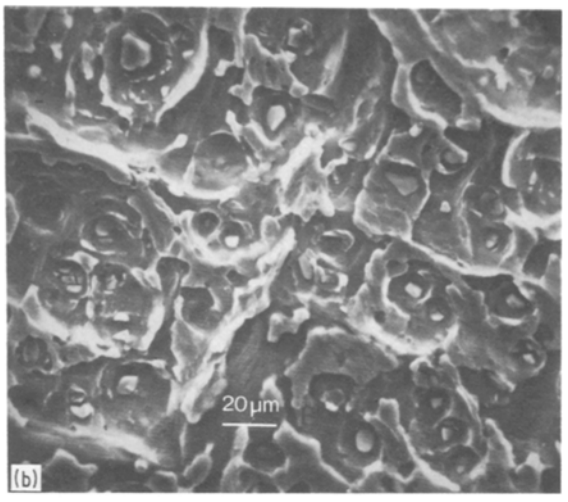

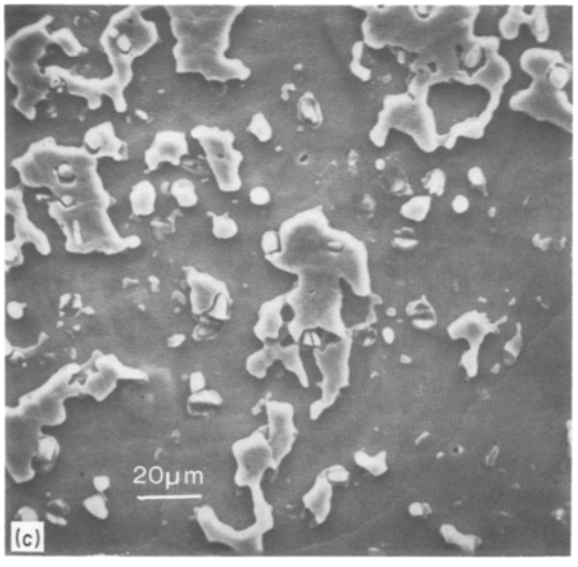

Figure 6 Scanning electron micrograph of 7010 alloy fracture surface: (a) interface between fractures produced in SHT (A) and aged (B) conditions, (b) fracture in SHT condition, (c) fracture in aged condition.

assumed to be little changed, but there was less plasticity in (2) and a significant increase in the stiffness of the test piece caused by the change from plastic to elastic deformation in (3). Since the rate of energy input was constant, ageing effectively increased the elastic strain energy in the test piece, which was dissipated largely by low ductility rapid fracture in the planar denuded grain boundaries. Similar low energy intergranular shear fractures have been observed in age hardened aluminium alloys [20]. This explains the high crack growth rates and the change in fracture mode for aged test pieces. The peel strengths in this condition were proportional to the clad layer thickness and inversely proportional to the clad layer hardness (Figs 11 and 12).

The flat low ductility fractures obtained at 480° C were unexpected considering the ductility of the alloys at this temperature. This fracture mode is attributed to lower crack growth resistance in the planar boundaries. The peel strengths at 480° C were $\leqslant 2.5\,\mathrm{N\,mm^{-1}}$ (Table II). These values indicate peel fracture of the diffusion bonded joint would occur during superplastic forming under gas pressure if the sheet thickness exceeded about 0.5 mm. Higher hot peel strengths are therefore required before thicker commercial aluminium sheets can be diffusion bonded and superplastically formed into the multiple sheet structures used for titanium [21]. However in two sheet structures thicker sheets could be diffusion bonded and formed using platen pressure as described elsewhere [18, 22].

In the present test programme the emphasis has

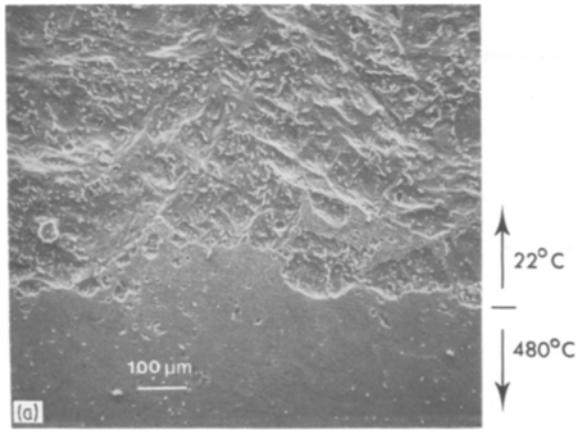

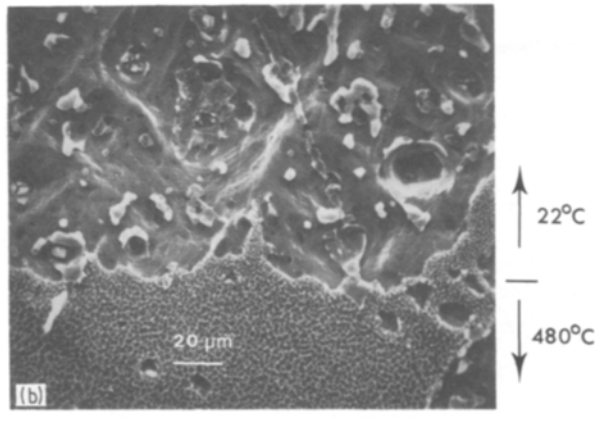

Figure 7 Scanning electron micrograph of 7010 alloy fracture surface: (a and b) interface between fracture produced at 22 and 480° C, (c) fracture at 22° C, (d) fracture at 480° C.

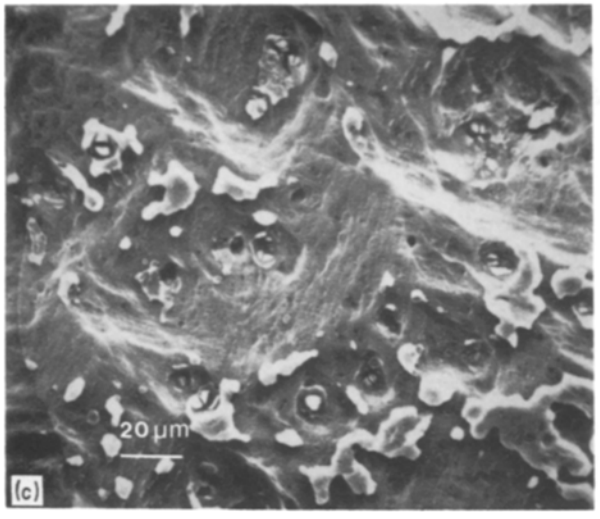

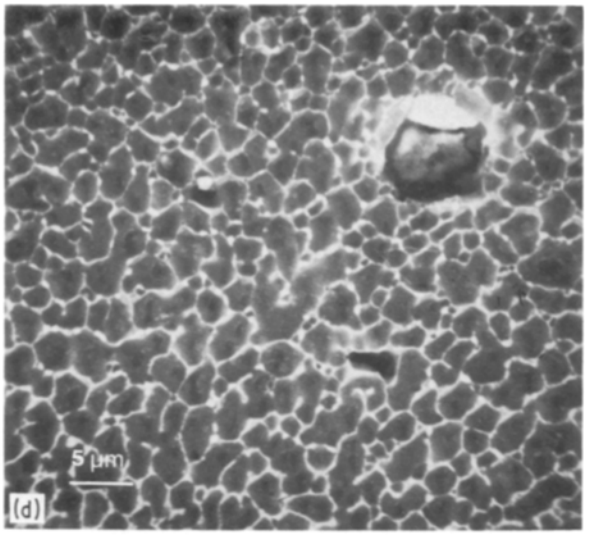

Figure 7 Continued

been on the peel test. In practice adhesive and diffusion bonded joints in structures are designed to carry only shear loads [23–25]. However high peel stresses can arise in overlap joints loaded in shear [25, 26] and this could explain the low failure loads reported [9] for diffusion bonded lap shear test pieces in the aged-condition.

5. Conclusions

1. The peel strengths of diffusion bonded joints between clad Al-alloy sheet at room temperature were 61 N mm^{-1} (7010 alloy), 42 N mm^{-1} (Supral 220 alloy) and 45 N mm^{-1} (2024 alloy) for material in the solution heat treated condition. The corresponding peel strengths in the aged condition were 34, 48 and 12 N mm^{-1}.

2. At 480° C the peel strengths were 2.4 N mm^{-1} (7010 alloy) 1.7 N mm^{-1} (Supral 220) and 2.5 N mm^{-1} (2024).

3. Microscopic ductile fractures were obtained in the solution heat treated condition and low energy intergranular fractures in the aged condition. Low ductility fracture surfaces were obtained at 480° C. The low ductility fracture planes occurred along the planar grain boundaries at the bond interface.

4. In the solution heat treated condition the peel strengths, which were dependent on the thickness and

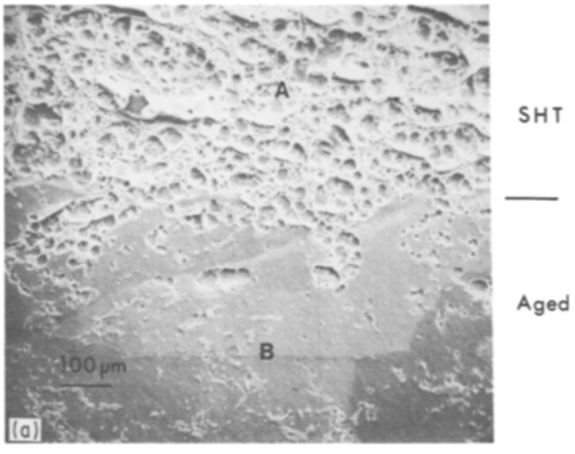

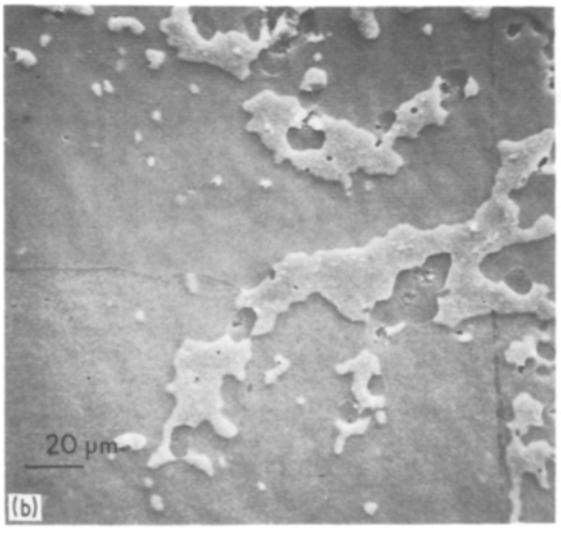

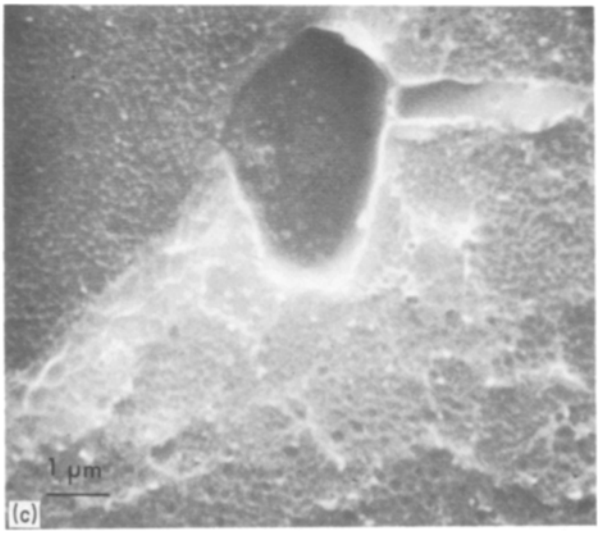

Figure 8 Scanning electron micrograph of Supral 220 alloy fracture surface. (a) interface between fracture produced in SHT (A) and aged (B) conditions, (b and c) fracture in aged condition.

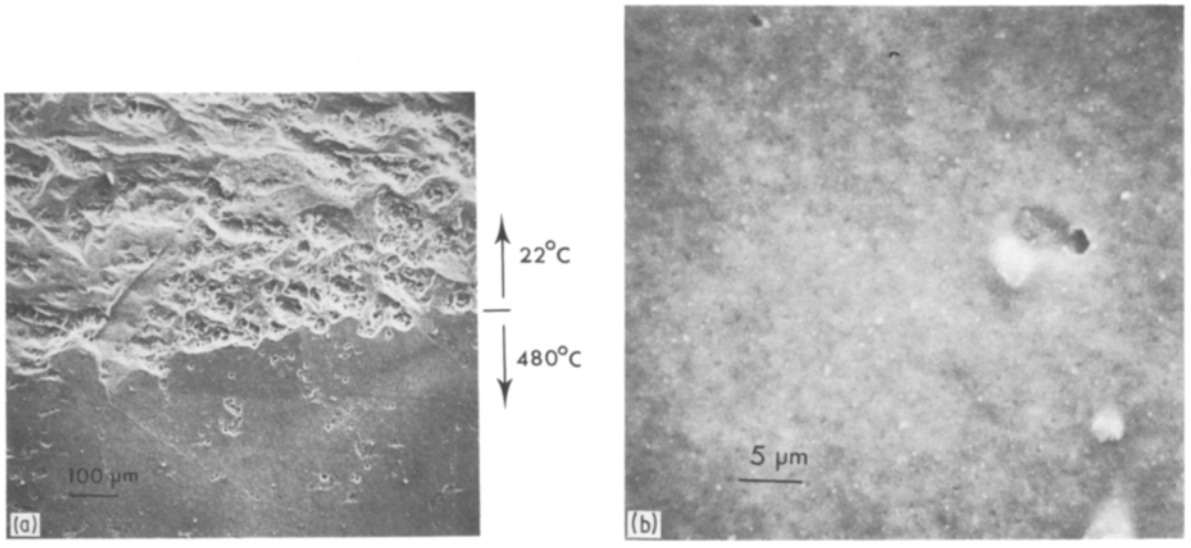

Figure 9 Scanning electron micrograph of Supral 220 alloy fracture surface: (a) interface between fracture produced at 22 and 480° C, (b) fracture at 480° C.

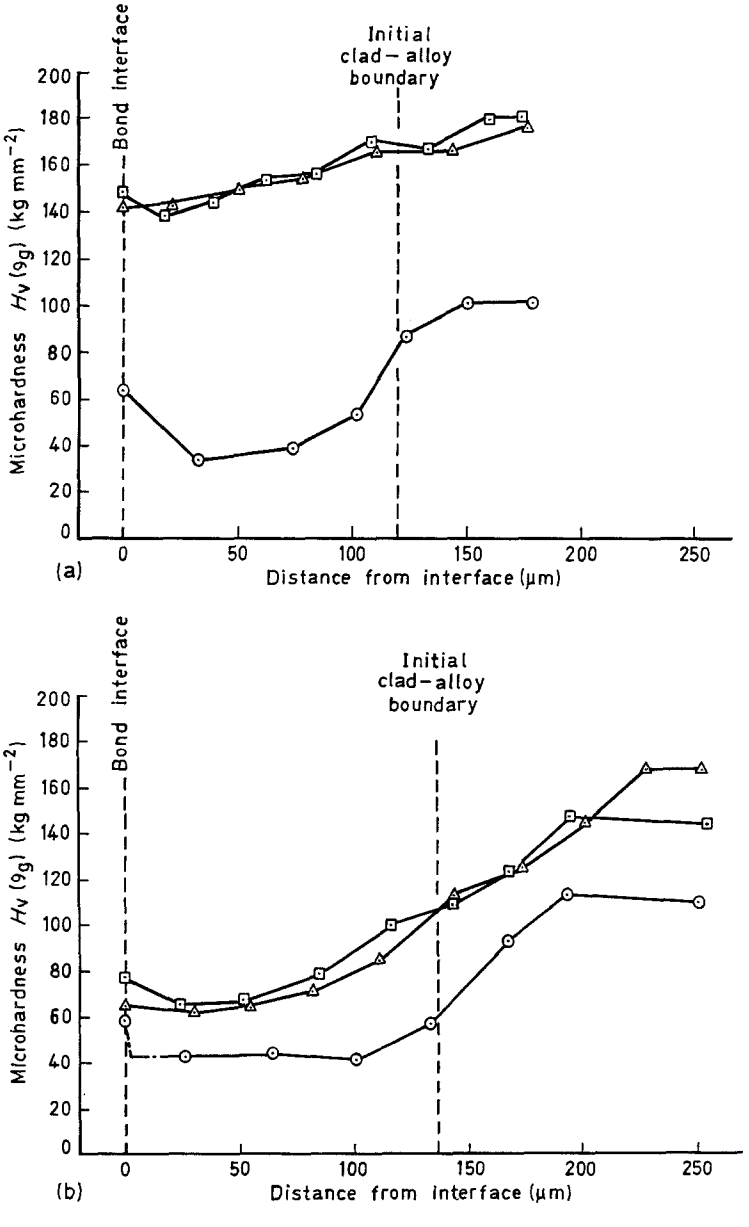

Figure 10 Microhardness values across bond interface: (a) 7010 alloy, (⊙) as-bonded, (□) SHT, (△) aged; (b) Supral 220 alloy, (○) as-bonded, (□) SHT, (△) aged; (c) 2024 alloy, (○) as-bonded, (□) SHT, (△) aged.

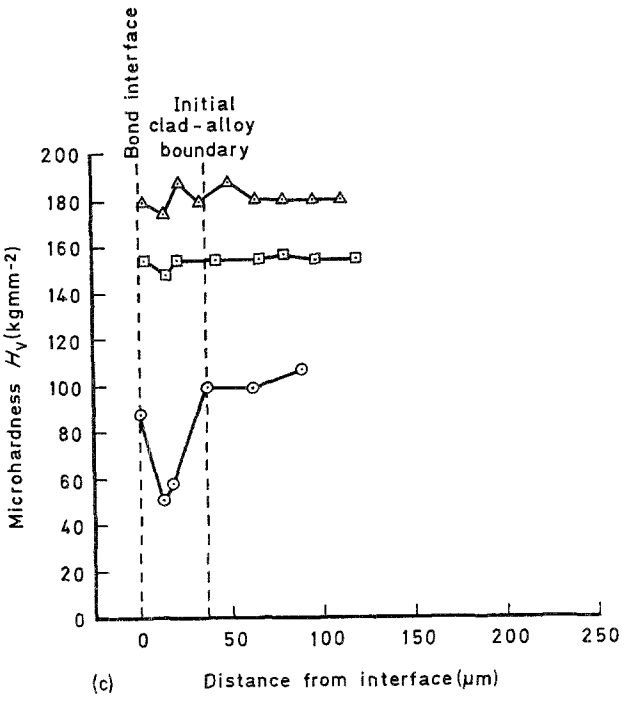

Figure 10 Continued

hardness of the clad layers, were attributed to the energy dissipated by plastic deformation.

5. In the aged condition the peel strengths appear to increase with increase in clad layer thickness and decrease in clad layer hardness.

6. The peel strengths at 480° C indicated peel fracture of the diffusion bonded joints would occur during superplastic forming if the sheet thickness was greater than about 0.5 mm.

Acknowledgement

This paper is published by the kind permission of the Royal Aircraft Establishment, Farnborough, UK. © Controller HMSO, London 1986.

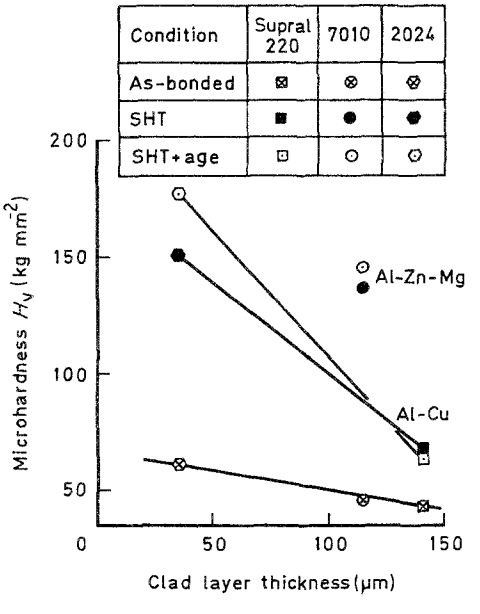

Figure 11 Hardness at 20 μm from the bond interface against clad layer thickness.

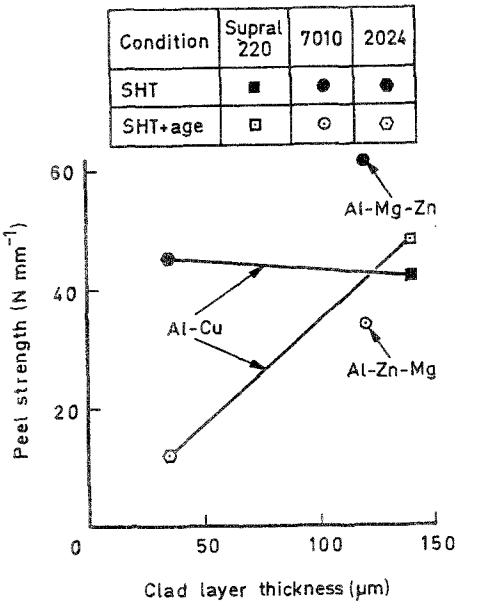

Figure 12 Peel strength against clad layer thickness.

References

1. "Advanced Aluminium and Titanium Structures", edited by J. Goodman, (American Society of Mechanical Engineers, Washington, November, 1981), p. 33.
2. *Idem, ibid.* p. 19.
3. C. L. CLINE, *Welding J. Suppl.* **45** (1966) 481s.
4. D. HAUSSER, D. A. KAMMER and J. H. DEDRICK, *ibid.* **46** (1967) 11s.
5. M. M. SCHWARTZ, "Metals Joining Manual" (McGraw-Hill, New York, 1979) p. 10–16.
6. I. M. BARTA, *Welding. Res. Suppl.* (1964) 241s.
7. P. G. PARTRIDGE, J. HARVEY and A. LURSHAY, *Mater. Sci. Eng.* **79** (1986) 191.
8. P. G. PARTRIDGE and A. J. SHAKESHEFF, RAE Technical Report 82117 (1982).
9. P. G. PARTRIDGE and D. V. DUNFORD, *ibid.* 86033 (1986).
10. D. V. DUNFORD and P. G. PARTRIDGE, unpublished work (1986).
11. R. J. SCHWENSFEIR Jr, G. TRENKLER, R. G. DELAGI and J. A. FORSTER, "Welding, Bonding and Fastening – 1984", (NASA Conference Publications, 2387, 1984) p. 323.
12. A. J. KINLOCH, *J. Mater. Sci.* **17** (1982) 617.
13. "Advanced Aluminium and Titanium Structures", American Society of Mechanical Engineers, Washington, November, 1981) p. 11.
14. R. E. BEAL, *J. Metals* **36** (November, 1984) 63.
15. G. J. GILMORE and P. G. PARTRIDGE, unpublished work (1986).
16. D. B. ARNOLD, "Developments in Adhesives – 2", (Applied Science, 1981) p. 207.
17. R. D. ADAMS and W. C. WAKE, "Structural Adhesive Joints in Engineering" (Elsevier Applied Science, 1984) p. 129.
18. D. V. DUNFORD and P. G. PARTRIDGE, Proceedings of the International Conference in "Superplasticity in Aerospace-Aluminium", Cranfield, July (Ashford Press, UK, 1985) p. 257.
19. P. G. PARTRIDGE and D. V. DUNFORD, *J. Mater. Sci.* **22** (1987).
20. W. W. GERBERICH, V. F. ZACKAY, E. R. PACKER and D. PORTER, "Ultrafine-grain Metals" (Syracuse University Press, New York, 1970). p. 259.
21. E. D. WEISERT and G. W. STACHER, "Superplastic Forming of Structural Alloys", AIME publication of Symposium, June 21–24, San Diego (1982) p. 273.
22. P. G. PARTRIDGE, J. HARVEY and D. V. DUNFORD, Advanced Joining of Metallic Materials, AGARD Conference Proceedings 389 AGARD, 1986, p. 81.

23. L. J. HART-SMITH, 19th National SAMPE Symposium (1974) p. 722.
24. *Idem*, "Delamination and Debonding of Materials", (ASTM STP 876, 1985) p. 238.
25. E. M. BREINAN and K. F. KREIDER, *Metals Eng. Quarterly* **9** (1969) 5.
26. G. E. METZGER, "Fabrication of Composite Materials", ASM (1985) p. 171.

Received 1 September
and accepted 9 September 1986